Process NMR Associates, LLC

Technical White Paper · PNA-WP-2026-RELAX-01

Optimum Pulse Tip Angle and Relaxation Delay for Selected Values of T_1

An Extended Ernst-Angle Chart, Quantitative-Recovery Tables, and a Relaxation-Delay Calculator for Pulsed Fourier-Transform NMR

John C. Edwards, Ph.D.

Process NMR Associates, LLC

84 Patrick Lane, Suite 115, Poughkeepsie, NY 12603

www.process-nmr.com

Version 1.0 · September 17, 2026

Document details

Document identifier	PNA-WP-2026-RELAX-01
Title	Optimum Pulse Tip Angle and Relaxation Delay for Selected Values of T_1
Version	1.0
Date of issue	September 17, 2026
Prepared by	Process NMR Associates, LLC (John C. Edwards, Ph.D.), 84 Patrick Lane, Suite 115, Poughkeepsie, NY 12603
Filename	PNA-WP-2026-RELAX-01_Tip_Angle_Relaxation_Delay_v1.0.docx
Companion files	PNA-WP-2026-RELAX-01_Companion_Workbook.xlsx (calculator, solver and all tables as live formulas); figure files Fig1–Fig5 in PDF and PNG
Model identity	claude-fable-5-1 (model identifier as reported by the session)
Generation date	2026-09-17
Tools engaged	Python 3.11 with NumPy, SciPy, Matplotlib and openpyxl (computation, figures, workbook); LibreOffice (formula recalculation and rendering); CrossRef REST API (verification of every reference); docx 9.6.1 on Node.js (document assembly)
AI-assistance statement	The theoretical framework, derivations, figures, tables, companion workbook and reference list of this document were drafted with AI assistance and were verified by independent recalculation of every numerical value and by resolution of every reference through CrossRef. Experimental relaxation times, instrument-specific parameters and the interpretation of results for any particular sample are supplied by Process NMR Associates and are not AI-generated.

Abstract

The choice of pulse tip angle and repetition time is the most consequential acquisition decision made in any pulsed Fourier-transform NMR experiment, and the relationships that govern it are treated here in a form intended for direct use at the spectrometer. The classic chart of optimum pulse width against pulse repetition rate for selected values of the spin–lattice relaxation time T_1, familiar from the instrument manuals of the 1970s, has been recomputed from the Ernst condition $\cos\theta_E = \exp(-T_R/T_1)$ and extended from 10 s to 20 s of repetition time for the same family of T_1 values (1, 2, 4, 6, 10, 15, 25 and 50 s). The reduced form of the same relationship, in which every curve collapses onto a single line in T_R/T_1, is presented alongside it. Because the Ernst condition maximizes sensitivity per unit time by deliberately accepting partial saturation, it is not the condition required for quantitative work, and a second relationship is therefore developed and tabulated: the repetition time at which steady-state longitudinal magnetization has recovered to within a stated tolerance ε of its equilibrium value for a given tip angle, $T_R = T_1 \cdot \ln[(1 - (1-\varepsilon)\cdot\cos\theta)/\varepsilon]$. This expression reduces to the familiar $4.6\cdot T_1$ and $6.9\cdot T_1$ at a 90° tip angle for tolerances of 1% and 0.1%, and to $2.66\cdot T_1$ at 30° and 1%, which is the basis for the use of reduced tip angles in quantitative NMR. The differential saturation that arises between an analyte and an internal standard of unequal T_1 is quantified, since it is this quantity rather than the recovery of any single resonance that governs the accuracy of a concentration determined from an integral ratio. A companion Microsoft Excel workbook is supplied in which the pulse tip angle, the acquisition time and the T_1 of the resonance are entered and the relaxation delay is returned under three criteria side by side, together with the steady-state recovery, the signal attenuation, the relative sensitivity per unit time, and the experiment duration; a second sheet evaluates and solves the two-component bias problem. Practical guidance on the measurement of T_1, the calibration of the tip angle, the establishment of the steady state, heteronuclear work under inverse-gated decoupling, and the use of relaxation agents is provided so that the tables can be applied with confidence.

Table of Contents

1. Introduction 4

2. Theory 4

2.1 Longitudinal recovery and the steady state under repetitive pulsing 4

2.2 The Ernst condition: maximum sensitivity per unit time 5

2.3 Recovery to a stated tolerance: the quantitative condition 6

2.4 The multiple-of-T_1 rule of thumb 6

2.5 Repetition time, acquisition time and the relaxation delay 7

3. The Extended Ernst-Angle Chart 7

3.1 Construction 7

3.2 Reading the chart 8

3.3 The reduced form 9

4. Repetition Time Required for Quantitative Recovery 10

5. Sensitivity per Unit Time and the Cost of Quantitation 12

6. Two Resonances with Different T_1: Differential Saturation 14

7. The Relaxation-Delay Calculator Workbook....16
7.1 The Calculator sheet....16
7.2 The three criteria side by side....17
7.3 The what-if block....17
7.4 The qNMR_Bias sheet....17
7.5 Lookup and data sheets....18
8. Practical Guidance for the Use of the Tables....18
8.1 Determining T_1 under the working conditions....18
8.2 Calibrating the tip angle....18
8.3 Establishing the steady state: dummy scans....19
8.4 Heteronuclear work under inverse-gated decoupling....19
8.5 Relaxation agents and the choice of internal standard....19
8.6 Choosing between the criteria....20
8.7 Recording the parameters....20
9. Worked Examples....20
9.1 Proton qNMR with an internal standard....20
9.2 Quantitative carbon-13 with and without a relaxation agent....20
9.3 A benchtop measurement....21
References....21
Summary....24

1. Introduction

Every pulsed Fourier-transform NMR experiment is a compromise between two quantities that pull in opposite directions. Signal is accumulated by repeating the excitation many times and averaging the transients, and the rate at which the signal-to-noise ratio improves with time is therefore fixed by how frequently the sample can be pulsed. Longitudinal magnetization, on the other hand, recovers toward its equilibrium value only at the rate set by the spin–lattice relaxation time T_1, and if the sample is pulsed again before recovery is complete, the magnetization available to the next pulse is diminished. The interplay between the tip angle of the pulse, the interval between pulses and the relaxation time of the nuclei was analyzed in the earliest work on Fourier-transform NMR by Ernst and Anderson, who showed that for any given repetition time there exists a tip angle at which the signal accumulated per unit time is maximized.[1–4] That angle has carried Ernst's name ever since, and the chart of optimum tip angle against repetition time for a family of T_1 values has been reproduced, in one form or another, in almost every spectrometer manual and NMR text published since.[5–8]

The purpose of the present paper is threefold. In the first place, the classic chart is recomputed from the underlying relationship and extended to a repetition time of 20 s, so that its coverage now embraces the slowly relaxing nuclei encountered in quantitative ^{13}C, ^{19}F, ^{29}Si and ^{31}P work as well as in degassed or dilute ^{1}H samples. In the second place, the distinct question of how long the repetition time must be for the measurement to be *quantitative* is addressed, and a relationship is developed and tabulated that credits the reduced saturation produced by a reduced tip angle rather than relying on the traditional multiple of T_1. In the third place, a calculator workbook is supplied in which the tip angle, the acquisition time and the relaxation time of the resonance of interest are entered and the relaxation delay to be set at the console is returned, together with the quantities needed to judge the cost of that choice in sensitivity and in spectrometer time.

The treatment is confined to the single-pulse experiment under steady-state conditions, which is the experiment on which all routine quantitative NMR is built.[9–12] The relationships presented are exact within the assumptions stated in Section 2, and the tables and figures have been computed directly from them rather than read from earlier charts. Where numerical values are quoted in the text they have been taken from the companion workbook, in which every quantity is a live formula, so that the reader may reproduce any number in this paper by entering the corresponding inputs.

2. Theory

2.1 Longitudinal recovery and the steady state under repetitive pulsing

Consider a spin system at thermal equilibrium with longitudinal magnetization M_0, subjected to a train of identical radiofrequency pulses of tip angle θ separated by a repetition time T_R. Immediately before each pulse the longitudinal magnetization has some value M_z^-; the pulse rotates it, leaving a longitudinal component $M_z^- \cdot \cos\theta$ and a transverse component $M_z^- \cdot \sin\theta$ that is detected as the free induction decay. During the interval T_R that follows, the longitudinal component recovers toward M_0 according to the Bloch equation, so that the magnetization presented to the next pulse is

$$M_z^-(\text{next}) = M_0 \cdot (1 - E_1) + M_z^- \cdot \cos\theta \cdot E_1, \qquad E_1 = \exp(-T_R/T_1) \tag{1}$$

After a number of pulses the magnetization before each pulse settles to a steady value at which the loss caused by the pulse is exactly balanced by the recovery during the interval. Setting the magnetization before successive pulses equal in Equation (1) and solving gives the steady-state longitudinal magnetization

$$M_z(ss) / M_0 = (1 - E_1) / (1 - E_1 \cdot \cos\theta) \quad (2)$$

and the observed signal, proportional to the transverse magnetization created by the pulse, is

$$S / S_0 = \sin\theta \cdot (1 - E_1) / (1 - E_1 \cdot \cos\theta) \quad (3)$$

in which S_0 is the signal that would be obtained from a single 90° pulse applied to a fully relaxed sample. Equations (2) and (3) are the foundation of everything that follows.[2,6,13] Their derivation assumes that the transverse magnetization has decayed completely before the next pulse arrives, so that no transverse coherence is carried from one pulse to the next. In high-resolution work the acquisition time is always several times T_2*, and this condition is satisfied automatically; where it is not, the steady state acquires a dependence on resonance offset and phase that was analyzed in detail by Freeman and Hill and that manifests itself as intensity and phase anomalies across the spectrum.[13] The derivation further assumes that the tip angle is the same for every spin in the detected volume and for every resonance in the spectrum, that the pulse is short relative to T_R, and that longitudinal recovery is described by a single exponential.

The approach to the steady state is itself of practical importance. Equation (1) is a linear recursion whose deviation from the steady state shrinks by the factor $E_1 \cdot \cos\theta$ at every pulse, so that after n pulses the residual deviation is $(E_1 \cdot \cos\theta)^n$ times the initial deviation $M_0 - M_z(ss)$. The first transient of a train is therefore always more intense than those that follow, and its inclusion in an averaged data set biases the integrals in a manner that Equations (2) and (3) do not describe. The remedy, which is the routine use of dummy scans before acquisition begins, is discussed in Section 8.3.

2.2 The Ernst condition: maximum sensitivity per unit time

If a fixed amount of spectrometer time is available, the number of transients that can be averaged is inversely proportional to T_R, and since the signal-to-noise ratio grows as the square root of the number of transients, the quantity to be maximized is $S/\sqrt{T_R}$.[1,7,14] For a fixed T_R the dependence on θ enters only through Equation (3), and differentiation with respect to θ shows that the signal is greatest when

$$\cos\theta_E = E_1 = \exp(-T_R/T_1) \quad (4)$$

This is the Ernst condition, and θ_E is the Ernst angle.[2,3] It has two properties that deserve emphasis. The first is that it depends on the repetition time and the relaxation time only through their ratio, so that a single curve of θ_E against T_R/T_1 contains the whole of the information in the family of curves drawn for particular values of T_1. The second is that the steady-state magnetization at the Ernst angle, obtained by substituting Equation (4) into Equation (2), is

$$M_z(ss) / M_0 = 1 / (1 + E_1) \quad (5)$$

which lies between one half and unity, and which equals 73.1% at $T_R = T_1$. The Ernst condition, in other words, is a condition of deliberate partial saturation. It maximizes the signal that can be accumulated in a given time by trading away a portion of the equilibrium magnetization in exchange for the right to pulse more often, and the signal that is observed under it is not proportional to the number of spins unless every resonance in the spectrum has the same T_1. It is the correct condition for a survey spectrum, for the detection

of a minor component, or for any measurement in which relative intensities within a spectrum are not the quantity sought.[6,15,16] It is not the condition for quantitation, and the distinction between the two is the subject of Section 2.3.

Inverted for the repetition time, Equation (4) gives the T_R at which a chosen tip angle becomes the optimum,

$$T_R(\text{Ernst}) = -T_1 \cdot \ln(\cos\theta) \tag{6}$$

which is finite for every tip angle below 90° and diverges as 90° is approached, reflecting the fact that a 90° pulse is the optimum only when the sample is allowed to relax completely between pulses.

2.3 Recovery to a stated tolerance: the quantitative condition

A measurement is quantitative when the integral of each resonance is proportional to the number of nuclei that give rise to it, and under repetitive pulsing that proportionality is preserved only if the steady-state magnetization of every resonance stands at the same fraction of its equilibrium value. The simplest way to guarantee this is to require that the fraction be close to unity for all of them, which is to say that the recovery described by Equation (2) be essentially complete.[9–11,17,18] If a tolerance ε is specified, such that $M_z(ss)/M_0$ must be at least $1 - \varepsilon$, then Equation (2) can be solved for E_1 and hence for the repetition time:

$$E_1 \le \varepsilon / [1 - (1-\varepsilon)\cdot\cos\theta] \tag{7}$$

$$T_R \ge T_1 \cdot \ln\{ [1 - (1-\varepsilon)\cdot\cos\theta] / \varepsilon \} \tag{8}$$

Equation (8) is the central result of this paper for quantitative work. At θ = 90° the cosine vanishes and the expression reduces to $T_R \ge T_1 \cdot \ln(1/\varepsilon)$, which gives $4.605 \cdot T_1$ for ε = 1% and $6.908 \cdot T_1$ for ε = 0.1%; the familiar rule of five times T_1 corresponds to a residual shortfall of 0.67%, and seven times T_1 to 0.091%.[6,7,19] As the tip angle is reduced the requirement falls, because a smaller pulse destroys less of the longitudinal magnetization and correspondingly less has to be recovered. At 45° and 1% the multiplier is 3.401; at 30° it is 2.658; at 20° it is 1.942; and at 10° it is 0.918. The use of a 30° pulse therefore permits the same 1% tolerance to be met in 47% less time per transient than the five-times-T_1 rule at 90°, and this is the whole of the argument for reduced tip angles in quantitative NMR.[12,15,16,20] The multiplier in Equation (8) depends only on θ and ε and not on T_1, so it is tabulated once in Section 4 and applied to any relaxation time by multiplication.

It should be noted that the tolerance ε in Equation (8) bounds the shortfall of a single resonance from full recovery, which is a common-mode attenuation that affects all resonances of the same T_1 equally. It does not by itself bound the accuracy of a ratio between two resonances whose relaxation times differ, and that quantity, which is the one that determines the accuracy of a concentration obtained by comparison with an internal standard, is treated separately in Section 6.

2.4 The multiple-of-T_1 rule of thumb

The rule that the repetition time should be five, or for the most exacting work seven or ten, times the longest relevant T_1 has been repeated in the quantitative NMR literature for half a century and is embedded in numerous standard methods.[17–19,21,22] Its virtue is simplicity: it is easily stated in a procedure, easily audited, and always sufficient. Its cost is that it takes no account of the tip angle. The rule was formulated for 90° excitation, where it corresponds to a tolerance of 0.67%, and when it is applied unchanged to a 30° pulse it delivers a recovery of 99.909%, or a tolerance of 0.091%, at the price of a repetition time nearly twice the

one that Equation (8) shows to be necessary for the 1% tolerance actually intended. The rule is retained in the companion workbook as one of the three criteria displayed, with the multiplier as an input, so that a method written around it can be evaluated on the same footing as the others.

2.5 Repetition time, acquisition time and the relaxation delay

The repetition time is not a parameter that is entered directly at most spectrometers. It is the sum of the pulse width, the acquisition time during which the free induction decay is digitized, and the relaxation delay that is inserted before the next pulse:

$$T_R = P_1 + AQ + D1 \tag{9}$$

The pulse width is of the order of microseconds and is neglected. The acquisition time is fixed by the spectral width and the number of points, and in high-resolution ^{1}H work it is commonly between two and five seconds; it is time during which relaxation proceeds exactly as it does during the delay, and it therefore counts in full toward T_R. The relaxation delay is the quantity that the operator sets, and it is obtained from any of the criteria above by subtraction:

$$D1 = T_R - AQ \tag{10}$$

When the acquisition time alone exceeds the required repetition time, the delay is set to zero and the effective repetition time is the acquisition time itself. That circumstance is common for rapidly relaxing ^{1}H resonances at reduced tip angles, and it is flagged explicitly by the companion workbook, which never returns a negative delay. The nomenclature varies between manufacturers; the relaxation delay is D1 on Bruker instruments and d1 on Varian and Agilent instruments, and the acquisition time is AQ and at respectively. The arithmetic is identical in every case.

3. The Extended Ernst-Angle Chart

3.1 Construction

Figure 1 presents the optimum tip angle as a function of pulse repetition rate for the eight values of T_1 used in the classic chart, with the repetition axis extended from 10 s to 20 s. Every curve was computed point by point from Equation (4) as $\theta_E = \arccos[\exp(-PR/T_1)]$, where PR denotes the pulse repetition rate in seconds and is identical to T_R, and none was traced from an earlier drawing. As a check on provenance, a digitized copy of the original chart was compared with the computed curves over the range it covered; the agreement was within the line width of the original drawing across the whole family. Figure 1 is therefore the same chart, drawn from its defining equation and carried to twice its former range. The values underlying it are tabulated at selected repetition rates in Table 1, and the full 0–20 s grid at 0.1 s intervals is available as live formulas on the Fig1_Data sheet of the companion workbook.

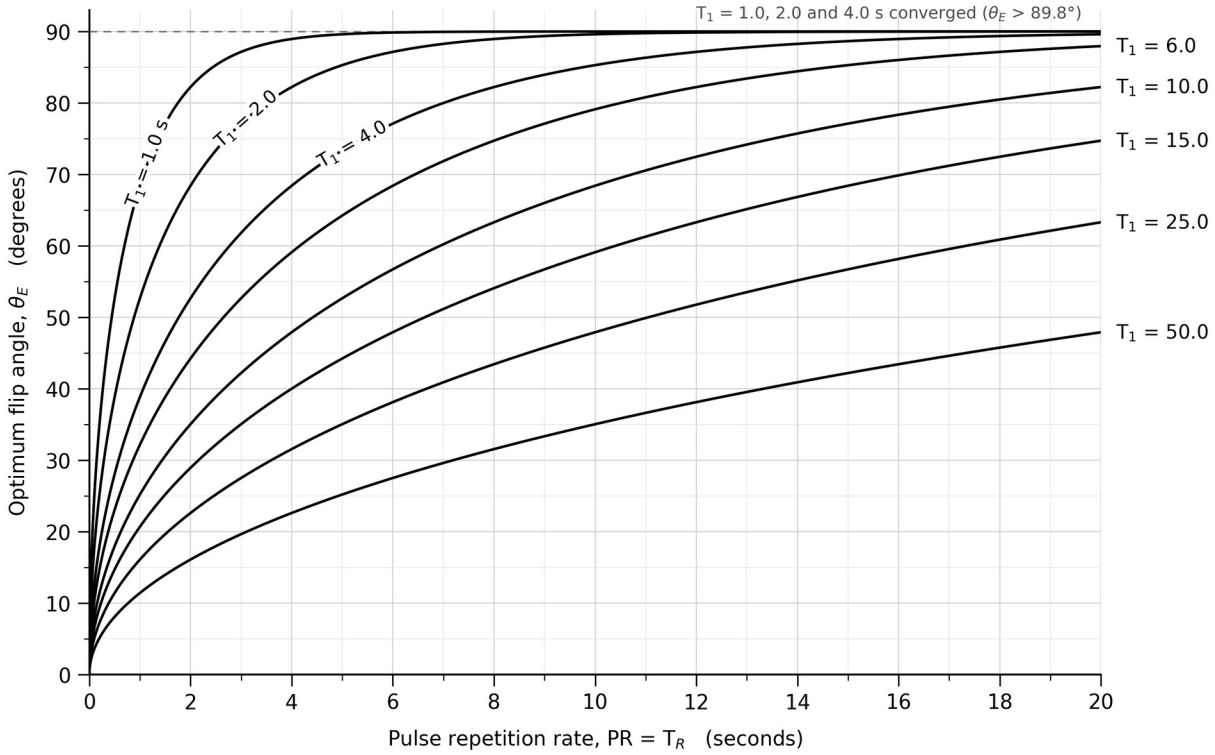

Figure 1. Optimum pulse tip angle θ_E against pulse repetition rate PR = T_R for T_1 = 1, 2, 4, 6, 10, 15, 25 and 50 s, computed from the Ernst condition $\cos\theta_E = \exp(-PR/T_1)$ and extended to 20 s. The three shortest-T_1 curves are labeled on their rising portions because they are indistinguishable from one another and from 90° beyond about 10 s.

Table 1. Optimum tip angle θ_E (degrees) at selected pulse repetition rates for the T_1 family of Figure 1.

T_1 (s)	0.5 s	1 s	2 s	3 s	4 s	5 s	6 s	8 s	10 s	12 s	15 s	20 s
1	52.7	68.4	82.2	87.1	89.0	89.6	89.9	90.0	90.0	90.0	90.0	90.0
2	38.8	52.7	68.4	77.1	82.2	85.3	87.1	89.0	89.6	89.9	90.0	90.0
4	28.1	38.8	52.7	61.8	68.4	73.4	77.1	82.2	85.3	87.1	88.7	89.6
6	23.1	32.2	44.2	52.7	59.1	64.2	68.4	74.7	79.1	82.2	85.3	88.0
10	18.0	25.2	35.0	42.2	47.9	52.7	56.7	63.3	68.4	72.5	77.1	82.2
15	14.7	20.7	28.9	35.0	40.0	44.2	47.9	54.1	59.1	63.3	68.4	74.7
25	11.4	16.1	22.6	27.5	31.6	35.0	38.1	43.4	47.9	51.8	56.7	63.3
50	8.1	11.4	16.1	19.6	22.6	25.2	27.5	31.6	35.0	38.1	42.2	47.9

3.2 Reading the chart

The chart is read by locating the curve for the relaxation time of the resonance of interest, moving along it to the repetition rate that the experiment will use, and reading the optimum tip angle from the vertical axis. For a resonance with T_1 = 6 s pulsed every 4 s, for example, the optimum is 59°; if the same resonance is pulsed every 10 s the optimum rises to 79°, and at 20 s it is 88°. Conversely, if the tip angle has been fixed by other considerations, the chart gives the repetition rate at which that angle is the best choice; a 45° pulse is optimal at a repetition rate of $0.35\cdot T_1$, and a 60° pulse at $0.69\cdot T_1$.

The extension of the axis to 20 s adds information only where the curves have not yet saturated. For T_1 = 1 s the optimum angle is within 0.1° of 90° by 6.4 s, and for T_1 = 2 s by 12.7 s, so the new territory of the chart is of use principally for relaxation times of six seconds and longer. Those are the relaxation times of quaternary carbons, of fluorine and silicon nuclei in small molecules, of phosphorus in many organophosphorus compounds, and of protons in degassed or very dilute solutions, and it is for those nuclei that the extended chart has been prepared.[17,23,24]

Because the optimum is a broad maximum, small departures from θ_E cost little. The signal function of Equation (3) falls by less than 2% for a departure of 10° on either side of the optimum over most of the chart, and this tolerance is the reason that the chart may be read to the nearest few degrees without loss.[6,7] It is also the reason that a reduced tip angle chosen for quantitative reasons, as in Section 4, is rarely far from the sensitivity optimum for the repetition time it entails.

3.3 The reduced form

Figure 2 shows the same relationship plotted against the dimensionless ratio T_R/T_1 on a logarithmic axis. Every curve of Figure 1 lies on this single line, and any combination of relaxation time and repetition time that is not represented in Figure 1 can be read from it by forming the ratio first. Table 2 tabulates the reduced curve together with the steady-state recovery, the signal relative to a fully relaxed 90° pulse, and the sensitivity per unit time at the Ernst point, each of which is a function of the ratio alone. The sensitivity column is normalized to its limiting value at vanishing repetition time, which is $1/\sqrt{2}$ in the units of Equation (3), and it shows that the sensitivity attainable under the Ernst condition declines steadily as the repetition time is lengthened: at $T_R = T_1$ it stands at 0.96 of the limit, at $2 \cdot T_1$ at 0.87, and at $5 \cdot T_1$ at 0.63.

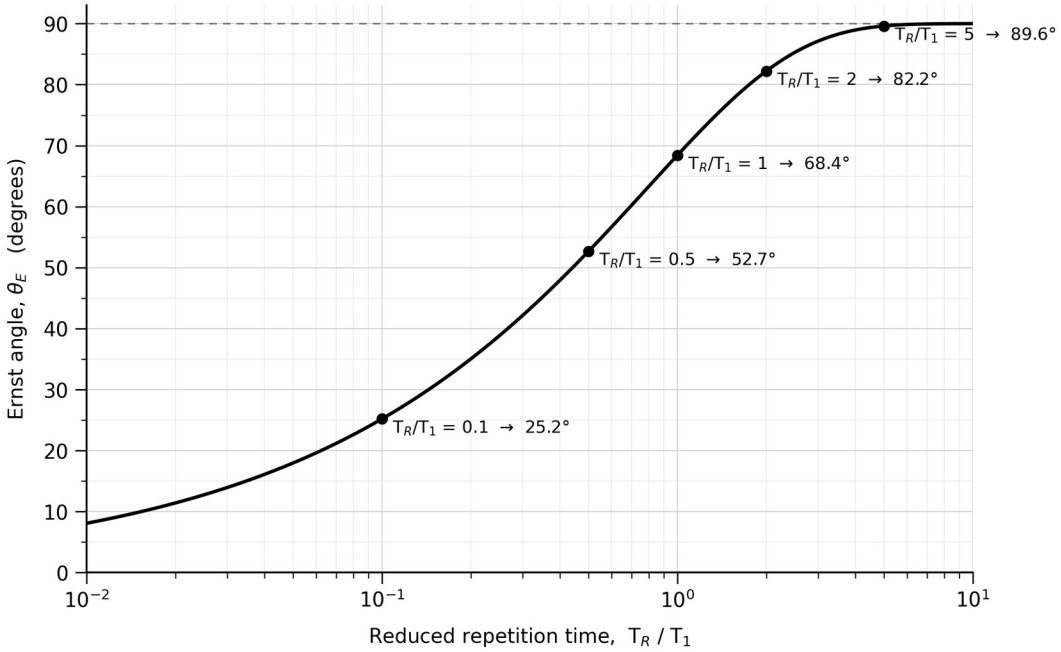

Figure 2. The Ernst condition in reduced form. The Ernst angle depends only on the ratio T_R/T_1, and the eight curves of Figure 1 are the single curve shown here with the abscissa rescaled by each T_1.

Table 2. The Ernst condition in reduced form: optimum angle, steady-state recovery, relative signal and relative sensitivity per unit time as functions of T_R/T_1.

T_R/T_1	θ_E (deg)	$M_z(ss)/M_0$ (%)	S/S_0 at θ_E	Sensitivity per √t (relative)
0.05	18.0	51.2	0.158	1.000
0.1	25.2	52.5	0.224	1.000
0.2	35.0	55.0	0.316	0.998
0.3	42.2	57.4	0.386	0.996
0.5	52.7	62.2	0.495	0.990
0.7	60.2	66.8	0.580	0.980
1	68.4	73.1	0.680	0.961
1.5	77.1	81.8	0.797	0.920
2	82.2	88.1	0.873	0.873
3	87.1	95.3	0.951	0.777
4	89.0	98.2	0.982	0.694
5	89.6	99.3	0.993	0.628
7	89.9	99.9	0.999	0.534
10	90.0	100.0	1.000	0.447

4. Repetition Time Required for Quantitative Recovery

Figure 3 plots the multiplier of Equation (8), the required T_R/T_1, against tip angle for four values of the recovery tolerance, and Table 3 tabulates it in five-degree steps at five tolerances. The classic five-times-T_1 level is marked on the figure, and the tip angle at which each tolerance curve crosses it may be read directly: the 0.1% curve crosses at about 32°, the 0.5% curve at about 75°, and the 1% curve does not reach it at any tip angle. Table 4 converts the 1% multiplier into repetition times in seconds for a grid of relaxation times and tip angles; the relaxation delay to be entered is obtained by subtracting the acquisition time from the tabulated value, as in Equation (10), and the companion workbook performs that subtraction for any combination of inputs.

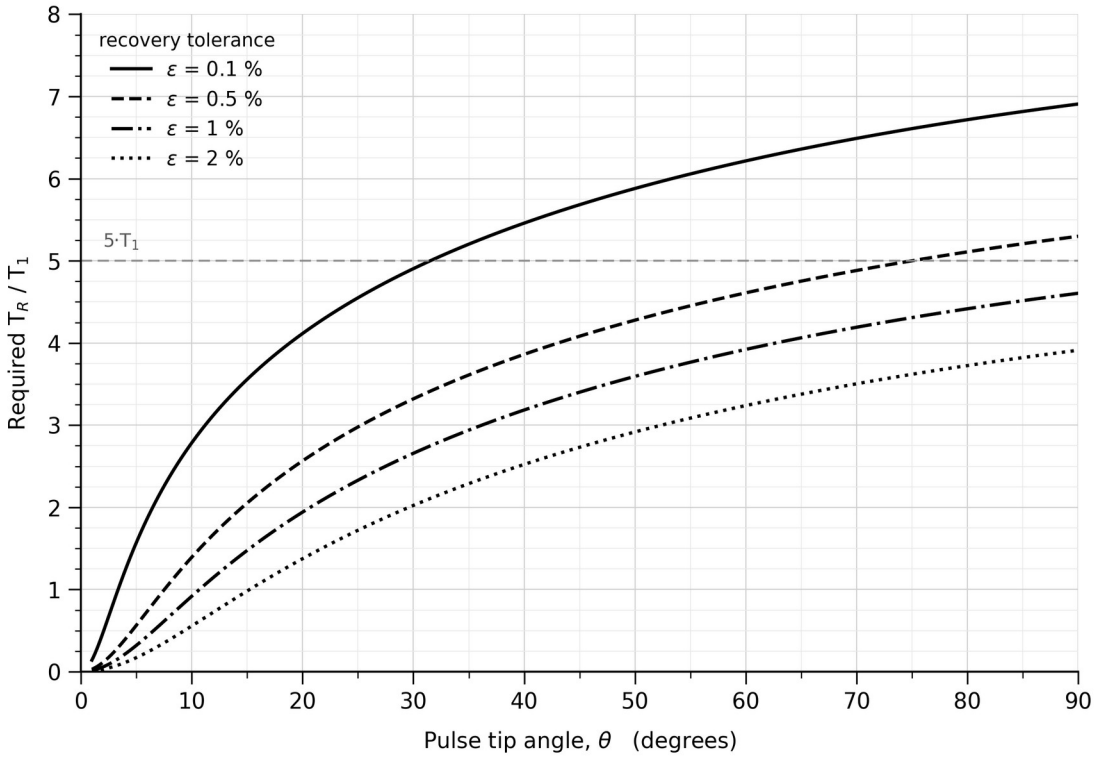

Figure 3. Repetition time required for steady-state recovery to $(1 - \varepsilon)\cdot M_0$, expressed as a multiple of T_1, against pulse tip angle for four tolerances, from Equation (8). The dashed line marks the traditional $5\cdot T_1$ rule.

Table 3. Required T_R/T_1 for steady-state recovery to $(1 - \varepsilon)\cdot M_0$ as a function of tip angle and tolerance, from Equation (8). The relaxation delay is D1 = (multiplier × T_1) − AQ.

θ (deg)	ε = 0.1%	ε = 0.5%	ε = 1%	ε = 2%	ε = 5%
5	1.569	0.564	0.320	0.171	0.070
10	2.784	1.392	0.918	0.556	0.254
15	3.556	2.052	1.476	0.982	0.499
20	4.115	2.565	1.942	1.375	0.764
25	4.550	2.978	2.330	1.721	1.023
30	4.904	3.320	2.658	2.023	1.266
35	5.202	3.611	2.939	2.289	1.490
40	5.458	3.862	3.185	2.523	1.695
45	5.682	4.082	3.401	2.731	1.882
50	5.880	4.278	3.594	2.918	2.052
55	6.057	4.453	3.766	3.086	2.208
60	6.216	4.610	3.922	3.239	2.351
65	6.359	4.753	4.063	3.377	2.482
70	6.490	4.882	4.192	3.504	2.603
75	6.609	5.001	4.309	3.619	2.714
80	6.717	5.109	4.417	3.725	2.815
85	6.817	5.208	4.515	3.823	2.909
90	6.908	5.298	4.605	3.912	2.996

Table 4. Required repetition time T_R in seconds at ε = 1% for selected relaxation times and tip angles. Subtract the acquisition time to obtain D1; a negative result means the acquisition time alone is sufficient and D1 = 0.

T_1 (s)	θ = 10°	θ = 20°	θ = 30°	θ = 45°	θ = 60°	θ = 75°	θ = 90°
0.5	0.46	0.97	1.33	1.70	1.96	2.15	2.30
1	0.92	1.94	2.66	3.40	3.92	4.31	4.61
1.5	1.38	2.91	3.99	5.10	5.88	6.46	6.91
2	1.84	3.88	5.32	6.80	7.84	8.62	9.21
3	2.75	5.83	7.97	10.20	11.77	12.93	13.82
4	3.67	7.77	10.63	13.60	15.69	17.24	18.42
5	4.59	9.71	13.29	17.01	19.61	21.55	23.03
6	5.51	11.65	15.95	20.41	23.53	25.85	27.63
8	7.34	15.53	21.26	27.21	31.38	34.47	36.84
10	9.18	19.42	26.58	34.01	39.22	43.09	46.05
15	13.77	29.13	39.87	51.02	58.83	64.64	69.08
20	18.36	38.83	53.15	68.02	78.44	86.18	92.10
30	27.54	58.25	79.73	102.03	117.66	129.27	138.16
50	45.90	97.08	132.89	170.05	196.10	215.46	230.26

Two features of Table 3 are worth drawing out. The first is the steepness of the dependence on tip angle at the low end. Between 90° and 45° the 1% multiplier falls by about a quarter, from 4.61 to 3.40; between 45° and 20° it falls by a further 43%, to 1.94; and at 10° it is below unity. The gain from reducing the tip angle is therefore greatest precisely in the range of angles, 20° to 45°, that is most often used in quantitative practice.[12,20,25] The second feature is that the spacing between the tolerance columns is nearly constant down the table, because Equation (8) is logarithmic in ε; each tenfold tightening of the tolerance adds approximately $2.3 \cdot T_1$ to the required repetition time regardless of the tip angle. A method that must hold 0.1% rather than 1% therefore pays the same additional time at 30° as it does at 90°, and the reduced tip angle preserves its advantage at every tolerance.

5. Sensitivity per Unit Time and the Cost of Quantitation

The sensitivity per unit time, $S/\sqrt{T_R}$, is plotted in Figure 5 against the reduced repetition time for five tip angles, together with the envelope traced by the Ernst condition, at which the tip angle is optimal at every repetition time. Each fixed-angle curve touches the envelope at the single repetition time for which that angle is the Ernst angle and falls away on either side; to the left, because the sample is over-saturated, and to the right, because time is being spent waiting for recovery that the small pulse does not require. The 90° curve is the least favorable at short repetition times and joins the envelope only as T_R becomes large relative to T_1, which is the graphical expression of Equation (6).[2,6,16]

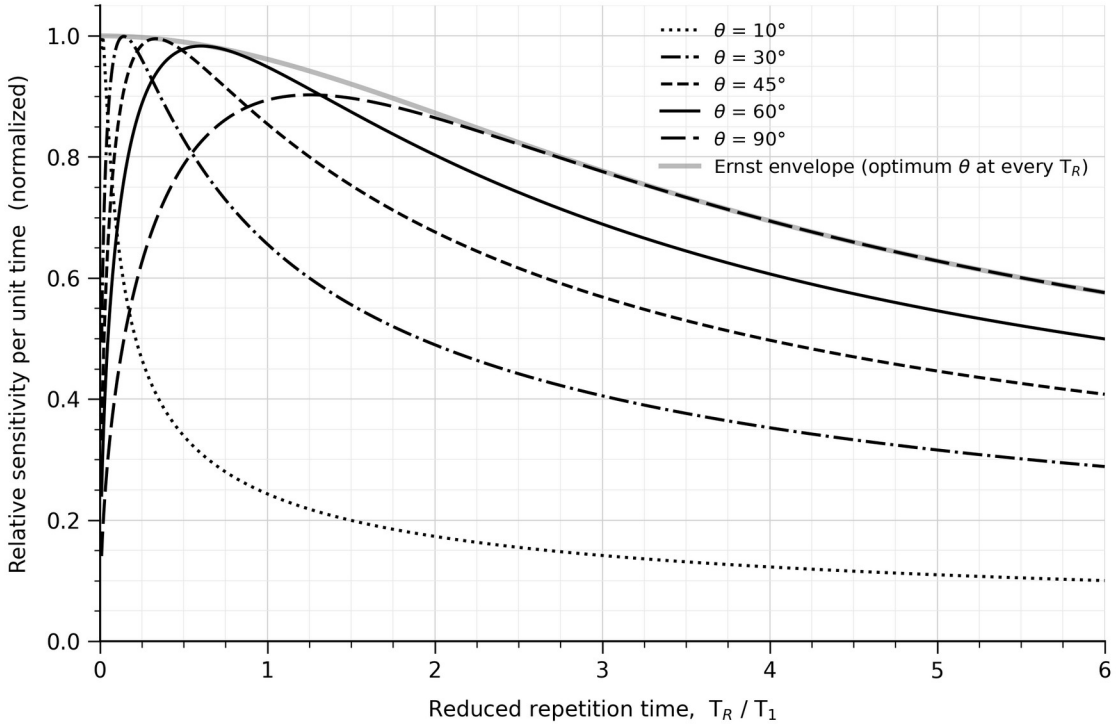

Figure 5. Relative sensitivity per unit time, $S/\sqrt{T_R}$ from Equation (3) normalized to its limiting value, against reduced repetition time for tip angles of 10°, 30°, 45°, 60° and 90°. The gray envelope is the Ernst condition. Each fixed-angle curve touches the envelope where that angle is the Ernst angle.

The figure makes the cost of quantitation explicit. A quantitative measurement is made at a point on one of the fixed-angle curves that lies well to the right of its maximum, and the vertical distance between that point and the envelope at the same repetition time is the sensitivity forgone. Because signal-to-noise ratio grows with the square root of measurement time, the ratio of the times required to reach equal noise is the inverse square of the ratio of sensitivities. Table 5 presents the worked example that is shipped as the default state of the companion workbook: a 30° tip angle, a 4.000 s acquisition time, a relaxation time of 5.000 s, a tolerance of 1%, and 64 transients. The four rows are the three criteria of Section 2 and, as a fourth, the Ernst optimum at the shortest repetition time the acquisition time permits, which is the fastest useful survey condition and the reference against which the sensitivities are normalized.

Table 5. Worked example at θ = 30°, AQ = 4.000 s, T_1 = 5.000 s, ε = 1%, n = 5 and 64 transients. T_R(eff) is the repetition time actually realized once the acquisition time is taken into account; sensitivity is normalized to the fourth row.

Criterion	T_R nominal (s)	D1 (s)	T_R(eff) (s)	T_R(eff)/T_1	M_z(ss)/M_0 (%)	S/S_0	Sensitivity per √t (rel.)	64 scans (h:mm:ss)
Flip-angle-compensated recovery, ε = 1%	13.289	9.289	13.289	2.658	99.000	0.4950	0.441	0:14:10
5 × T_1 rule	25.000	21.000	25.000	5.000	99.909	0.4995	0.324	0:26:40
Ernst condition at θ = 30°	0.719	0.000	4.000	0.800	90.145	0.4507	0.731	0:04:16
Ernst optimum at T_R = AQ (θ_E = 63.3°)	4.000	0.000	4.000	0.800	68.997	0.6164	1.000	0:04:16

The example repays study. The quantitative condition requires a relaxation delay of 9.29 s and a repetition time of 13.29 s, at which the steady-state recovery is 99.00% by construction and the sensitivity per unit time is 0.441 of the survey optimum, so that 5.2 times the survey measurement time is required to reach the same noise level. The five-times-T_1 rule requires 21.00 s of delay and 25.00 s of repetition time, delivers a recovery of 99.909% that exceeds what was asked for, and returns a sensitivity of 0.324, so that 1.85 times as long is needed as under the tolerance criterion for the same signal-to-noise. The Ernst condition at 30° calls for a repetition time of only 0.719 s, which is shorter than the acquisition time and therefore cannot be realized; the shortest attainable repetition time is the acquisition time itself, at which a 30° pulse is no longer optimal and the Ernst angle is 63.3°. Sixty-four transients occupy 0:14:10 under the quantitative condition, 0:26:40 under the five-times-T_1 rule, and 0:04:16 under the survey condition.

6. Two Resonances with Different T_1: Differential Saturation

When a concentration is determined by comparing the integral of an analyte resonance with that of an internal standard, the quantity that enters the calculation is a ratio, and any factor common to both integrals cancels. The recovery tolerance of Section 4 bounds the common-mode attenuation, and if the analyte and the standard had the same relaxation time the ratio would be exact at any repetition time whatsoever. They rarely do. Internal standards are chosen for chemical stability, spectral simplicity and the absence of overlap, and their relaxation times are what they are; the small, rigid molecules that make good standards frequently relax faster than the analyte, and sometimes much faster.[26–30] The bias that results is obtained directly from Equation (3) applied to each species:

$$\text{bias} = \left[(1 - E_a) / (1 - E_a \cdot \cos\theta) \right] / \left[(1 - E_s) / (1 - E_s \cdot \cos\theta) \right] - 1 \qquad (11)$$

$$E_a = \exp(-T_R/T_{1a}), \quad E_s = \exp(-T_R/T_{1s})$$

in which the subscripts a and s denote the analyte and the standard. The sine factor cancels because the tip angle is common to both, so the bias depends on the tip angle only through the denominators. Equation (11) is negative when the analyte relaxes more slowly than the standard, in which case the analyte integral is under-recovered relative to the standard and the concentration reported from the ratio is low by the same fraction; it is positive in the opposite case. In the limit of very short repetition time the bias tends to the ratio $T_{1s}/T_{1a} - 1$, which for a standard relaxing three times faster than the analyte is a bias of −67%, and it decays toward zero as the repetition time is lengthened.[18,25,31]

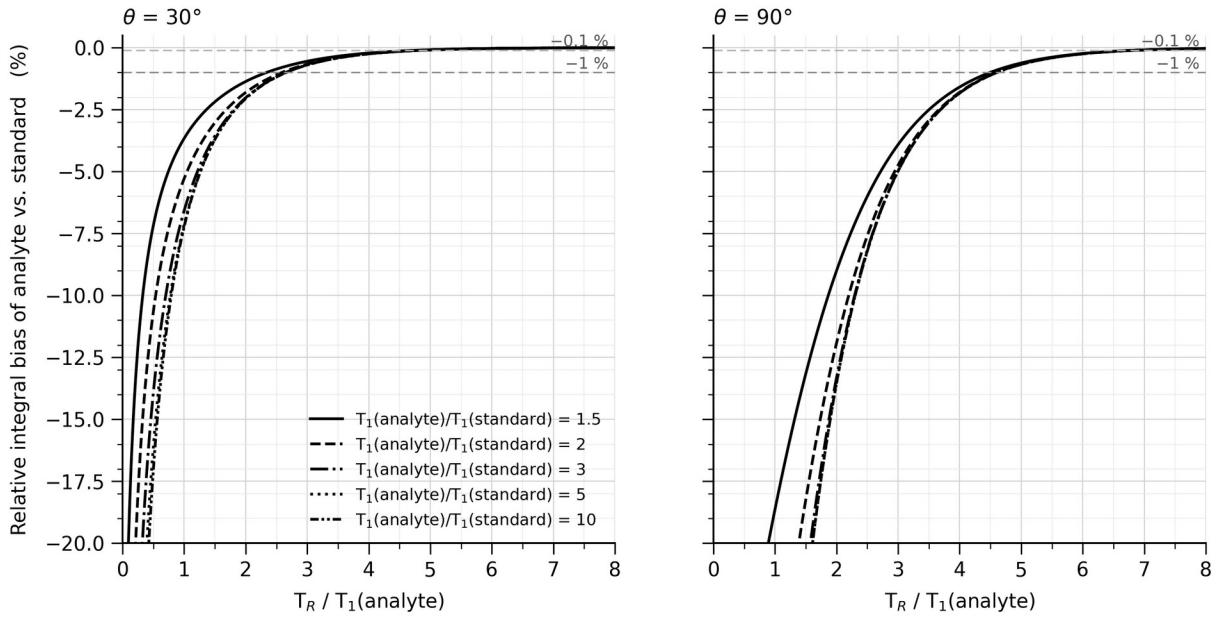

Figure 4. Relative bias of the analyte integral against that of a faster-relaxing internal standard, from Equation (11), as a function of T_R/T_1(analyte) for five ratios of the two relaxation times, at tip angles of 30° (left) and 90° (right). The dashed lines mark biases of −1% and −0.1%.

Figure 4 plots Equation (11) for five ratios of the relaxation times at tip angles of 30° and 90°, and Table 6 tabulates the same curves. Several conclusions follow. The bias is governed almost entirely by the slower of the two species: once the ratio of relaxation times exceeds about three, the curves become nearly indistinguishable, because the standard is by then fully recovered at any repetition time that gives the analyte a reasonable recovery, and the bias is simply the shortfall of the analyte alone. A tip angle of 30° brings the bias inside 1% at a repetition time of about $2.7 \cdot T_1$(analyte) for a threefold ratio, whereas 90° requires about $4.6 \cdot T_1$(analyte), which is the advantage of Section 4 carried over intact to the ratio. And the bias inside the 1% line decays slowly, so that reaching 0.1% costs a further $2.3 \cdot T_1$(analyte) at either angle, exactly as the logarithmic form of Equation (8) predicts for the single-resonance case.

Table 6a. Relative integral bias (%) of the analyte against a faster-relaxing internal standard at θ = 30°, from Equation (11), as a function of T_R/T_1(analyte) and of the ratio T_1(analyte)/T_1(standard).

T_R/T_1(analyte)	ratio 1.5	ratio 2	ratio 3	ratio 5	ratio 10
1	-3.663	-5.288	-6.582	-7.149	-7.232
1.5	-2.185	-3.029	-3.560	-3.698	-3.705
2	-1.366	-1.809	-2.021	-2.053	-2.054
2.5	-0.865	-1.094	-1.177	-1.184	-1.184
3	-0.548	-0.664	-0.695	-0.697	-0.697
4	-0.216	-0.245	-0.249	-0.249	-0.249
5	-0.083	-0.090	-0.091	-0.091	-0.091
6	-0.032	-0.033	-0.033	-0.033	-0.033
7	-0.012	-0.012	-0.012	-0.012	-0.012

Table 6b. Relative integral bias (%) of the analyte against a faster-relaxing internal standard at θ = 90°, from Equation (11), as a function of T_R/T_1(analyte) and of the ratio T_1(analyte)/T_1(standard).

T_R/T_1(analyte)	ratio 1.5	ratio 2	ratio 3	ratio 5	ratio 10
1	-18.632	-26.894	-33.476	-36.359	-36.785
1.5	-13.160	-18.243	-21.440	-22.270	-22.313
2	-9.003	-11.920	-13.319	-13.530	-13.534
2.5	-5.998	-7.586	-8.158	-8.208	-8.208
3	-3.911	-4.743	-4.967	-4.979	-4.979
4	-1.588	-1.799	-1.831	-1.832	-1.832
5	-0.619	-0.669	-0.674	-0.674	-0.674
6	-0.236	-0.247	-0.248	-0.248	-0.248
7	-0.088	-0.091	-0.091	-0.091	-0.091

A rigorous bound on the repetition time required to hold the bias inside a target can be written in closed form by applying Equation (8) to the longer of the two relaxation times with a slightly tightened tolerance ε′ = target/(1 + target); at that repetition time the slower species has recovered to 1 − ε′ and the faster species to at least that, so the ratio cannot deviate from unity by more than the target in either direction. The companion workbook reports this bound alongside an exact solution obtained by searching a fine grid of repetition times, and the two are displayed together so that the search can be checked against the closed form.

Three remedies exist when the bias is found to be unacceptable at the repetition time the method can afford. The repetition time may be lengthened, which is always effective and always the slowest option. A standard may be chosen whose relaxation time more nearly matches that of the analyte, which is why the relaxation times of candidate internal standards are reported in the qualification studies of Rundlöf and of Wells and their co-workers.[26,27] Or a paramagnetic relaxation agent may be added to draw all relaxation times down toward a common short value, which is discussed in Section 8.5. A fourth course, which is to measure the saturation factor for each species and correct the integrals arithmetically, is legitimate provided the relaxation times are measured and reported and the steady state is demonstrably reached, but it places the accuracy of the result entirely on the accuracy of the relaxation-time determination.[25,31] External referencing methods, in which the standard is not present in the sample, remove one of the two relaxation times from the ratio altogether and leave only the recovery of the analyte to be assured.[28,32–34]

7. The Relaxation-Delay Calculator Workbook

The companion workbook, PNA-WP-2026-RELAX-01_Companion_Workbook.xlsx, implements every relationship in this paper as a live formula. It contains no hard-coded results, every input cell is identified by blue text on a pale yellow background, and every formula has been recalculated and compared cell by cell against an independent implementation of Equations (2) through (11) before release. The workbook is arranged in eleven sheets, which are described in turn.

7.1 The Calculator sheet

Three primary inputs are entered: the pulse tip angle in degrees, the acquisition time in seconds, and the spin–lattice relaxation time in seconds of the resonance of interest, which should be the longest relevant T_1 in the sample. Three secondary parameters follow with sensible defaults: the recovery tolerance ε, the

multiplier n for the multiple-of-T_1 rule, and the number of transients, which is used only to compute the experiment duration. The primary result block returns the repetition time required by Equation (8), the relaxation delay obtained from it by Equation (10), the same repetition time expressed as a multiple of T_1, and the steady-state recovery actually achieved. When the acquisition time alone exceeds the required repetition time, the delay is reported as zero and a note states that the effective repetition time is the acquisition time.

7.2 The three criteria side by side

Below the primary result a table presents four rows: the tolerance criterion of Equation (8), the multiple-of-T_1 rule, the Ernst condition of Equation (6) at the entered tip angle, and the Ernst optimum at the shortest repetition time the acquisition time permits. For each row the nominal repetition time, the relaxation delay, the effective repetition time, its ratio to T_1, the steady-state recovery, the signal relative to a fully relaxed 90° pulse, the sensitivity per unit time normalized to the fourth row, and the total experiment time for the entered number of transients are displayed, together with a remark that states in words what the row means. Table 5 of this paper is that block at the shipped default values.

7.3 The what-if block

A separate block accepts a relaxation delay that has already been chosen, or that is prescribed by an existing procedure, and reports the repetition time that results, the steady-state recovery, the signal relative to full recovery, the shortfall expressed as a percentage, and the Ernst angle corresponding to that repetition time. A message states whether the chosen delay meets the tolerance set in the inputs and, if it does not, by how much it falls short. This block is intended for the review of methods written before the tables in this paper were available. For use away from the workbook, Table 7 tabulates the steady-state recovery of Equation (2) against reduced repetition time and tip angle, so that the recovery delivered by an existing delay can be read directly once the ratio of repetition time to relaxation time has been formed.

Table 7. Steady-state recovery $M_z(ss)/M_0$ (%) as a function of reduced repetition time T_R/T_1 and tip angle, from Equation (2).

T_R/T_1	θ = 10°	θ = 20°	θ = 30°	θ = 45°	θ = 60°	θ = 90°
0.5	97.71	91.49	82.88	68.89	56.47	39.35
1	99.12	96.61	92.77	85.44	77.46	63.21
1.5	99.57	98.30	96.29	92.24	87.44	77.69
2	99.76	99.06	97.95	95.62	92.74	86.47
2.5	99.86	99.46	98.82	97.45	95.72	91.79
3	99.92	99.69	99.30	98.49	97.45	95.02
4	99.97	99.89	99.75	99.46	99.08	98.17
5	99.99	99.96	99.91	99.80	99.66	99.33
7	100.00	99.99	99.99	99.97	99.95	99.91

7.4 The qNMR_Bias sheet

The two-component sheet accepts the relaxation times of the analyte and of the internal standard, the tip angle, the acquisition time, the relaxation delay in use, and a target for the ratio bias. It returns Equation (11) evaluated at the delay in use, states in words whether the analyte integral is biased high or low and by how

much, and then solves for the shortest repetition time at which the bias falls inside the target. The solution is found by searching a grid of fifteen hundred repetition times spanning up to fifteen times the longer relaxation time, and it is reported together with the closed-form bound described in Section 6 and the grid resolution, so that the answer can be audited. The relaxation times, tip angle and acquisition time are linked to the Calculator sheet by default and may be overwritten to decouple the two sheets.

7.5 Lookup and data sheets

The D1_Table sheet presents the relaxation delay across a grid of twenty relaxation times and eighteen tip angles at the tolerance and acquisition time set on the Calculator sheet, together with the tip-angle multiplier of Equation (8) as a single row. The Fig1_Data and Fig3_Data sheets carry the numerical data of Figures 1 and 3 at fine intervals. The sheets Table1 through Table7 reproduce, as formulas, the tables of this paper, and Table 4 in particular carries its tolerance as an editable cell so that the grid may be regenerated at any tolerance. A README sheet states the equations, the assumptions and the color conventions.

8. Practical Guidance for the Use of the Tables

8.1 Determining T_1 under the working conditions

Every table in this paper takes T_1 as an input, and the value used must be the relaxation time of the resonances in the sample as it will actually be measured. Relaxation times are sensitive to temperature, to viscosity, to concentration, to the presence of dissolved oxygen, and above all to traces of paramagnetic species, and a value taken from a different solvent, a different preparation or the literature is not a substitute for one measured in the sample at hand.[19,23,35] The inversion–recovery experiment of Vold and co-workers remains the reference method, and a determination at eight to twelve recovery delays spanning about five times the expected T_1 with a fully relaxed repetition time is neither long nor difficult for a modern instrument.[23,36–38] Where time is short, the saturation–recovery, progressive-saturation and fast inversion–recovery variants give serviceable values at a fraction of the cost, and the annotated bibliography of Kingsley is a convenient guide to the choice among them.[35,39–42] For the purposes of the tables the relaxation time to be entered is the longest among the resonances that will be integrated, or, on the two-component sheet, the two relaxation times individually.

It is prudent to determine T_1 on the instrument that will be used for the measurement. For small molecules in the extreme-narrowing regime the relaxation time is nearly independent of the field, but that regime is not guaranteed for larger or more viscous systems, and relaxation contributions from chemical-shift anisotropy scale with the square of the field. A relaxation time measured on a 60 MHz benchtop instrument is the correct input for a method run on that instrument, and the arithmetic of the tables is unchanged by the field.

8.2 Calibrating the tip angle

The tip angle entered into the tables is the nominal angle, and the tables assume that it is realized uniformly throughout the detected volume. The 90° pulse width should be calibrated on the sample, or on a sample of matched ionic strength and volume, by the usual nutation array, and the reduced pulse obtained by proportion.[8,43] The calibration is more consequential at reduced tip angles than at 90° because the signal function of Equation (3) varies more steeply with θ there; but the recovery criterion of Equation (8) is forgiving of small errors, since a pulse that is somewhat larger than nominal is somewhat more saturating

and a delay computed for the nominal angle then delivers a recovery slightly below the tolerance rather than grossly so. In an internal-standard measurement any inhomogeneity of the radiofrequency field is experienced identically by analyte and standard, and its effect on the ratio is of second order.

8.3 Establishing the steady state: dummy scans

As noted in Section 2.1, the first transients of a pulse train are not at steady state, and their deviation from it decays by the factor $E_1 \cdot \cos\theta$ at each pulse. Under the quantitative condition of Equation (8) the factor is small; at 30° and 1% it is 0.061, so that two dummy scans reduce the initial deviation to 0.37% of its value and four to a negligible amount. Under survey conditions the factor is larger; at the Ernst angle it equals E_1^2, which at $T_R = T_1$ is 0.135 and requires four or more dummy scans before the residual falls below 1%. Dummy scans are inexpensive and their omission is one of the commonest sources of integral bias in otherwise well-designed measurements; they should be run at the working repetition time, with the same tip angle and acquisition parameters as the transients that follow.[13,20,44]

8.4 Heteronuclear work under inverse-gated decoupling

For quantitative ^{13}C, ^{31}P and ^{29}Si work under proton decoupling, the nuclear Overhauser enhancement must be suppressed, and the standard means of doing so is to gate the decoupler on only during acquisition.[17,24,45,46] The enhancement nevertheless begins to build during the acquisition period, and it decays during the relaxation delay at a rate governed by the longitudinal relaxation of the observed nucleus. Because the maximum enhancement for a ^{13}C nucleus relaxed by dipolar coupling to protons is nearly twice the equilibrium magnetization, a residual enhancement that is a small fraction of its maximum can nonetheless be a significant fraction of the signal, and it is differential between protonated and quaternary carbons. The delay required to suppress it is therefore somewhat longer than the delay required for recovery alone at the same tolerance, and the long-standing recommendation of five to ten times the longest ^{13}C T_1 for inverse-gated quantitative work reflects that requirement.[24,47–49] The tables of this paper give the recovery component of the delay; the enhancement component is met by a modest extension, and the two are met together, at far lower cost, when a relaxation agent is used.

8.5 Relaxation agents and the choice of internal standard

Paramagnetic relaxation agents, of which chromium(III) acetylacetonate is the most widely used, shorten the longitudinal relaxation of every nucleus in the sample toward a common value set by the electron–nuclear interaction, and at the same time quench the nuclear Overhauser enhancement by providing a relaxation pathway that does not involve the protons.[24,49–51] Their use converts a ^{13}C measurement that would otherwise require a repetition time of minutes into one that requires seconds, and it compresses the spread of relaxation times that gives rise to the differential bias of Section 6. The concentration must be chosen so that the relaxation times are shortened without broadening the resonances beyond what the resolution of the measurement can accept, and the agent must be inert toward the analyte; a determination of T_1 after its addition is the proper input to the tables. For ^{1}H work the agent is used less often, because proton relaxation times are already short and the resulting broadening is more objectionable, and the preferred remedy for a mismatch between analyte and standard is the selection of a standard whose relaxation time is closer to that of the analyte, guided by the published qualification studies.[20,26,27]

8.6 Choosing between the criteria

The criterion to be applied follows from the purpose of the measurement. When the spectrum is acquired to identify what is present, to confirm a structure, or to detect a minor component, the Ernst condition is the correct choice and Figure 1 or Figure 2 gives the tip angle for whatever repetition time is convenient; the acquisition time alone is frequently sufficient, and the Ernst angle at that repetition time is reported by the fourth row of the Calculator sheet. When integrals are to be compared with one another or with a standard, Equation (8) is the criterion, with the tolerance set from the accuracy the method must hold and the tip angle chosen in the 20° to 45° range that Table 3 shows to be most economical; the two-component sheet is then used to confirm that the ratio bias against the standard is acceptable. When a method is being written for a laboratory in which auditability matters more than throughput, the multiple-of-T_1 rule remains defensible, and its cost relative to the tolerance criterion can be read from the workbook so that the choice is made knowingly.[18,19,22,30,52]

8.7 Recording the parameters

A quantitative result is only as reproducible as the record of the conditions under which it was obtained. The relaxation time on which the delay was based, the method by which it was measured, the tip angle and its calibration, the acquisition time, the relaxation delay, the number of dummy scans, the tolerance adopted and the resulting steady-state recovery are all quantities that a reviewer, an auditor or a second laboratory attempting to reproduce the measurement will require, and the Calculator sheet is arranged so that a printed copy of it constitutes that record.[18,19,53,54]

9. Worked Examples

9.1 Proton qNMR with an internal standard

An analyte resonance has been found by inversion–recovery to have T_1 = 5.0 s, and the singlet of the internal standard to have T_1 = 2.0 s. A 30° pulse and a 4.0 s acquisition time are to be used. Equation (8) at a 1% tolerance gives a repetition time of 13.29 s for the analyte and a relaxation delay of 9.29 s. At that repetition time the standard has recovered to 99.983% and the ratio bias from Equation (11) is -0.98%, which is essentially the tolerance itself because the standard is fully recovered and the analyte is not. If the method must hold 0.5%, the two-component solver returns a repetition time of 16.60 s and a delay of 12.60 s; for 0.1% it returns 24.6 s and a delay of 20.6 s. Sixty-four transients at the 1% condition occupy 0:14:10, and at the 0.1% condition 0:26:11. A five-times-T_1 rule applied to the analyte would set the repetition time at 25 s and the delay at 21 s, and would hold the bias to -0.09%.

9.2 Quantitative carbon-13 with and without a relaxation agent

A quaternary aromatic carbon in a small molecule has T_1 = 30 s, and a quantitative ^{13}C spectrum is required under inverse-gated decoupling with a 30° pulse and a 1.5 s acquisition time. Equation (8) at 1% gives a repetition time of 79.7 s and a delay of 78.2 s for recovery alone, and the extension of Section 8.4 for suppression of the residual enhancement would carry the delay toward two or three minutes. Two hundred and fifty-six transients at the recovery condition alone would occupy 5:40:11. If chromium(III) acetylacetonate is added at a concentration that brings the longest carbon relaxation time to 2.0 s, which is representative of the values obtained at concentrations in the tens of millimolar, the same criterion gives a

repetition time of 5.32 s and a delay of 3.82 s, the enhancement is quenched, and the same number of transients occupies 0:22:41. For a survey spectrum of the same sample without the agent, in which protonated carbons with T_1 near 3 s are the signals of interest and the acquisition time alone is used as the repetition time, Figure 2 gives an Ernst angle of 53°.

9.3 A benchtop measurement

On a 60 MHz benchtop instrument the acquisition time is typically shorter than at high field, because the linewidth attainable does not reward long acquisition, and the relaxation delay consequently carries a larger share of the repetition time. If the longest relaxation time in a sample has been measured on the benchtop instrument as 3.5 s and a 45° pulse with a 1.6 s acquisition time is used, Equation (8) at 1% gives a repetition time of 11.90 s and a delay of 10.30 s; at 0.5% the repetition time is 14.29 s. The reduced signal per transient of a low-field instrument makes the sensitivity forgone by the quantitative condition, which Table 5 illustrates, more keenly felt, and the economy of a reduced tip angle correspondingly more valuable: the same 1% tolerance at 90° would require 16.12 s, or 35% longer per transient.

References

1. Ernst, R. R. Sensitivity Enhancement in Magnetic Resonance. I. Analysis of the Method of Time Averaging. *Rev. Sci. Instrum.* **1965**, *36*, 1689–1695. https://doi.org/10.1063/1.1719443
2. Ernst, R. R.; Anderson, W. A. Application of Fourier Transform Spectroscopy to Magnetic Resonance. *Rev. Sci. Instrum.* **1966**, *37*, 93–102. https://doi.org/10.1063/1.1719961
3. Ernst, R. R. Sensitivity Enhancement in Magnetic Resonance. *Adv. Magn. Reson.* **1966**, *2*, 1–135. https://doi.org/10.1016/b978-1-4832-3115-0.50008-9
4. Ernst, R. R. Nuclear Magnetic Resonance Fourier Transform Spectroscopy (Nobel Lecture). *Angew. Chem., Int. Ed. Engl.* **1992**, *31*, 805–823. https://doi.org/10.1002/anie.199208053
5. Waugh, J. S. Sensitivity in Fourier transform NMR spectroscopy of slowly relaxing systems. *J. Mol. Spectrosc.* **1970**, *35*, 298–305. https://doi.org/10.1016/0022-2852(70)90205-5
6. Becker, E. D.; Ferretti, J. A.; Gambhir, P. N. Selection of optimum parameters for pulse Fourier transform nuclear magnetic resonance. *Anal. Chem.* **1979**, *51*, 1413–1420. https://doi.org/10.1021/ac50045a016
7. Rabenstein, D. L. Sensitivity enhancement by signal averaging in pulsed/Fourier transform NMR spectroscopy. *J. Chem. Educ.* **1984**, *61*, 909. https://doi.org/10.1021/ed061p909
8. Claridge, T. D. W. *High-Resolution NMR Techniques in Organic Chemistry*, 3rd ed.; Elsevier: Amsterdam, 2016. https://doi.org/10.1016/C2015-0-04654-8
9. Jungnickel, J. L.; Forbes, J. W. Quantitative Measurement of Hydrogen Types by Intergrated Nuclear Magnetic Resonance Intensities. *Anal. Chem.* **1963**, *35*, 938–942. https://doi.org/10.1021/ac60201a005
10. Hollis, D. P. Quantitative Analysis of Aspirin, Phenacetin, and Caffeine Mixtures by Nuclear Magnetic Resonance Spectrometry. *Anal. Chem.* **1963**, *35*, 1682–1684. https://doi.org/10.1021/ac60204a043
11. Pauli, G. F.; Jaki, B. U.; Lankin, D. C. Quantitative ^{1}H NMR: Development and Potential of a Method for Natural Products Analysis. *J. Nat. Prod.* **2005**, *68*, 133–149. https://doi.org/10.1021/np0497301
12. Bharti, S. K.; Roy, R. Quantitative ^{1}H NMR spectroscopy. *TrAC, Trends Anal. Chem.* **2012**, *35*, 5–26. https://doi.org/10.1016/j.trac.2012.02.007
13. Freeman, R.; Hill, H. D. W. Phase and intensity anomalies in Fourier transform NMR. *J. Magn. Reson.* **1971**, *4*, 366–383. https://doi.org/10.1016/0022-2364(71)90047-3

14. Hoult, D. I.; Richards, R. E. The signal-to-noise ratio of the nuclear magnetic resonance experiment. *J. Magn. Reson.* **1976**, *24*, 71–85. https://doi.org/10.1016/0022-2364(76)90233-x

15. Traficante, D. D. Optimum tip angle and relaxation delay for quantitative analysis. *Concepts Magn. Reson.* **1992**, *4*, 153–160. https://doi.org/10.1002/cmr.1820040204

16. Traficante, D. D.; Steward, L. R. The relationship between sensitivity and integral accuracy further comments on optimum tip angle and relaxation delay for quantitative analysis. *Concepts Magn. Reson.* **1994**, *6*, 131–135. https://doi.org/10.1002/cmr.1820060204

17. Shoolery, J. N. Some quantitative applications of ^{13}C NMR spectroscopy. *Prog. Nucl. Magn. Reson. Spectrosc.* **1977**, *11*, 79–93. https://doi.org/10.1016/0079-6565(77)80003-4

18. Malz, F.; Jancke, H. Validation of quantitative NMR. *J. Pharm. Biomed. Anal.* **2005**, *38*, 813–823. https://doi.org/10.1016/j.jpba.2005.01.043

19. Saito, T.; Nakaie, S.; Kinoshita, M.; Ihara, T.; Kinugasa, S.; Nomura, A.; Maeda, T. Practical guide for accurate quantitative solution state NMR analysis. *Metrologia* **2004**, *41*, 213–218. https://doi.org/10.1088/0026-1394/41/3/015

20. Pauli, G. F.; Gödecke, T.; Jaki, B. U.; Lankin, D. C. Quantitative ^{1}H NMR. Development and Potential of an Analytical Method: An Update. *J. Nat. Prod.* **2012**, *75*, 834–851. https://doi.org/10.1021/np200993k

21. Holzgrabe, U.; Deubner, R.; Schollmayer, C.; Waibel, B. Quantitative NMR spectroscopy—Applications in drug analysis. *J. Pharm. Biomed. Anal.* **2005**, *38*, 806–812. https://doi.org/10.1016/j.jpba.2005.01.050

22. ASTM International. ASTM D5292-99(2014), *Standard Test Method for Aromatic Carbon Contents of Hydrocarbon Oils by High Resolution Nuclear Magnetic Resonance Spectroscopy*; ASTM International: West Conshohocken, PA, 2014. https://doi.org/10.1520/D5292-99R14

23. Levy, G. C.; Peat, I. R. The experimental approach to accurate carbon-13 spin-lattice relaxation measurements. *J. Magn. Reson.* **1975**, *18*, 500–521. https://doi.org/10.1016/0022-2364(75)90106-7

24. Cookson, D. J.; Smith, B. E. Optimal conditions for obtaining quantitative ^{13}C NMR data. *J. Magn. Reson.* **1984**, *57*, 355–368. https://doi.org/10.1016/0022-2364(84)90253-1

25. Giraudeau, P. Challenges and perspectives in quantitative NMR. *Magn. Reson. Chem.* **2017**, *55*, 61–69. https://doi.org/10.1002/mrc.4475

26. Rundlöf, T.; Mathiasson, M.; Bekiroglu, S.; Hakkarainen, B.; Bowden, T.; Arvidsson, T. Survey and qualification of internal standards for quantification by ^{1}H NMR spectroscopy. *J. Pharm. Biomed. Anal.* **2010**, *52*, 645–651. https://doi.org/10.1016/j.jpba.2010.02.007

27. Wells, R. J.; Cheung, J.; Hook, J. M. Dimethylsulfone as a universal standard for analysis of organics by QNMR. *Accredit. Qual. Assur.* **2004**, *9*, 450–456. https://doi.org/10.1007/s00769-004-0779-0

28. Cullen, C. H.; Ray, G. J.; Szabo, C. M. A comparison of quantitative nuclear magnetic resonance methods: internal, external, and electronic referencing. *Magn. Reson. Chem.* **2013**, *51*, 705–713. https://doi.org/10.1002/mrc.4004

29. Schoenberger, T. Determination of standard sample purity using the high-precision ^{1}H-NMR process. *Anal. Bioanal. Chem.* **2012**, *403*, 247–254. https://doi.org/10.1007/s00216-012-5777-1

30. Weber, M.; Hellriegel, C.; Rueck, A.; Wuethrich, J.; Jenks, P. Using high-performance ^{1}H NMR (HP-qNMR®) for the certification of organic reference materials under accreditation guidelines—Describing the overall process with focus on homogeneity and stability assessment. *J. Pharm. Biomed. Anal.* **2014**, *93*, 102–110. https://doi.org/10.1016/j.jpba.2013.09.007

31. Le Gresley, A.; Fardus, F.; Warren, J. Bias and Uncertainty in Non-Ideal qNMR Analysis. *Crit. Rev. Anal. Chem.* **2015**, *45*, 300–310. https://doi.org/10.1080/10408347.2014.944971

32. Burton, I. W.; Quilliam, M. A.; Walter, J. A. Quantitative ^{1}H NMR with External Standards: Use in Preparation of Calibration Solutions for Algal Toxins and Other Natural Products. *Anal. Chem.* **2005**, *77*, 3123–3131. https://doi.org/10.1021/ac048385h

33. Wider, G.; Dreier, L. Measuring Protein Concentrations by NMR Spectroscopy. *J. Am. Chem. Soc.* **2006**, *128*, 2571–2576. https://doi.org/10.1021/ja055336t

34. Akoka, S.; Barantin, L.; Trierweiler, M. Concentration Measurement by Proton NMR Using the ERETIC Method. *Anal. Chem.* **1999**, *71*, 2554–2557. https://doi.org/10.1021/ac981422i

35. Kingsley, P. B. Methods of measuring spin-lattice (T_1) relaxation times: An annotated bibliography. *Concepts Magn. Reson.* **1999**, *11*, 243–276. https://doi.org/10.1002/(sici)1099-0534(1999)11:4<243::aid-cmr5>3.0.co;2-c

36. Vold, R. L.; Waugh, J. S.; Klein, M. P.; Phelps, D. E. Measurement of Spin Relaxation in Complex Systems. *J. Chem. Phys.* **1968**, *48*, 3831–3832. https://doi.org/10.1063/1.1669699

37. Christensen, K. A.; Grant, D. M.; Schulman, E. M.; Walling, C. Optimal determination of relaxation times of Fourier transform nuclear magnetic resonance. Determination of spin-lattice relaxation times in chemically polarized species. *J. Phys. Chem.* **1974**, *78*, 1971–1977. https://doi.org/10.1021/j100612a022

38. Weiss, G. H.; Gupta, R. K.; Ferretti, J. A.; Becker, E. D. The choice of optimal parameters for measurement of spin-lattice relaxation times. I. Mathematical formulation. *J. Magn. Reson.* **1980**, *37*, 369–379. https://doi.org/10.1016/0022-2364(80)90044-x

39. Freeman, R.; Hill, H. D. W. Fourier Transform Study of NMR Spin–Lattice Relaxation by "Progressive Saturation". *J. Chem. Phys.* **1971**, *54*, 3367–3377. https://doi.org/10.1063/1.1675352

40. McDonald, G. G.; Leigh, J. S. A new method for measuring longitudinal relaxation times. *J. Magn. Reson.* **1973**, *9*, 358–362. https://doi.org/10.1016/0022-2364(73)90177-7

41. Look, D. C.; Locker, D. R. Time Saving in Measurement of NMR and EPR Relaxation Times. *Rev. Sci. Instrum.* **1970**, *41*, 250–251. https://doi.org/10.1063/1.1684482

42. Canet, D.; Levy, G. C.; Peat, I. R. Time saving in ^{13}C spin-lattice relaxation measurements by inversion-recovery. *J. Magn. Reson.* **1975**, *18*, 199–204. https://doi.org/10.1016/0022-2364(75)90238-3

43. Keifer, P. A. 90° pulse width calibrations: How to read a pulse width array. *Concepts Magn. Reson.* **1999**, *11*, 165–180. https://doi.org/10.1002/(sici)1099-0534(1999)11:3<165::aid-cmr4>3.0.co;2-d

44. Torres, A. M.; Price, W. S. Common problems and artifacts encountered in solution-state NMR experiments. *Concepts Magn. Reson., Part A* **2016**, *45A*, e21387. https://doi.org/10.1002/cmr.a.21387

45. Freeman, R.; Hill, H. D. W.; Kaptein, R. Proton-decoupled NMR spectra of carbon-13 with the nuclear Overhauser effect suppressed. *J. Magn. Reson.* **1972**, *7*, 327–329. https://doi.org/10.1016/0022-2364(72)90194-1

46. Sotak, C. H.; Dumoulin, C. L.; Levy, G. C. Software for quantitative analysis by carbon-13 Fourier transform nuclear magnetic resonance spectrometry. *Anal. Chem.* **1983**, *55*, 782–787. https://doi.org/10.1021/ac00255a043

47. Caytan, E.; Remaud, G. S.; Tenailleau, E.; Akoka, S. Precise and accurate quantitative ^{13}C NMR with reduced experimental time. *Talanta* **2007**, *71*, 1016–1021. https://doi.org/10.1016/j.talanta.2006.05.075

48. Tenailleau, E.; Akoka, S. Adiabatic ^{1}H decoupling scheme for very accurate intensity measurements in ^{13}C NMR. *J. Magn. Reson.* **2007**, *185*, 50–58. https://doi.org/10.1016/j.jmr.2006.11.007

49. Otte, D. A. L.; Borchmann, D. E.; Lin, C.; Weck, M.; Woerpel, K. A. ^{13}C NMR Spectroscopy for the Quantitative Determination of Compound Ratios and Polymer End Groups. *Org. Lett.* **2014**, *16*, 1566–1569. https://doi.org/10.1021/ol403776k

50. Gansow, O. A.; Burke, A. R.; La Mar, G. N. A shiftless relaxation reagent for carbon-13 magnetic resonance of organometallic carbonyl compounds. *J. Chem. Soc., Chem. Commun.* **1972**, 456–457. https://doi.org/10.1039/c39720000456

51. Levy, G. C.; Komoroski, R. A. Paramagnetic relaxation reagents. Alternatives or complements to lanthanide shift reagents in nuclear magnetic resonance spectral analysis. *J. Am. Chem. Soc.* **1974**, *96*, 678–681. https://doi.org/10.1021/ja00810a007

52. Holzgrabe, U. Quantitative NMR spectroscopy in pharmaceutical applications. *Prog. Nucl. Magn. Reson. Spectrosc.* **2010**, *57*, 229–240. https://doi.org/10.1016/j.pnmrs.2010.05.001

53. Pauli, G. F.; Chen, S.-N.; Simmler, C.; Lankin, D. C.; Gödecke, T.; Jaki, B. U.; Friesen, J. B.; McAlpine, J. B.; Napolitano, J. G. Importance of Purity Evaluation and the Potential of Quantitative ^{1}H NMR as a Purity Assay. *J. Med. Chem.* **2014**, *57*, 9220–9231. https://doi.org/10.1021/jm500734a

54. Simmler, C.; Napolitano, J. G.; McAlpine, J. B.; Chen, S.-N.; Pauli, G. F. Universal quantitative NMR analysis of complex natural samples. *Curr. Opin. Biotechnol.* **2014**, *25*, 51–59. https://doi.org/10.1016/j.copbio.2013.08.004

Summary

The relationships that govern the choice of pulse tip angle and repetition time in pulsed Fourier-transform NMR have been set out in a form intended for direct application, and the classic chart of optimum tip angle against repetition rate for relaxation times of 1 to 50 s has been recomputed from the Ernst condition and extended to 20 s. The extension adds information for relaxation times of about six seconds and longer, which are those of quaternary carbons, of fluorine, silicon and phosphorus nuclei in small molecules, and of protons in degassed or dilute solutions; for shorter relaxation times the optimum angle has already reached 90° within the range of the original chart. The reduced form of the same relationship, a single curve in T_R/T_1, has been presented and tabulated so that any combination of relaxation time and repetition time may be evaluated.

The Ernst condition maximizes sensitivity per unit time by accepting partial saturation, and the steady-state magnetization under it lies between one half and unity of the equilibrium value. It is the appropriate condition for survey and detection work and is not a quantitative condition. For quantitative work the repetition time required for steady-state recovery to within a tolerance ε has been derived as $T_R = T_1 \cdot \ln[(1 - (1-\varepsilon)\cdot\cos\theta)/\varepsilon]$, which reduces to the familiar multiples of T_1 at 90° and falls to $2.66 \cdot T_1$ at 30° for a 1% tolerance. The multiplier has been tabulated against tip angle at five tolerances, and repetition times in seconds have been tabulated for a grid of relaxation times at 1%. Each tenfold tightening of the tolerance adds approximately $2.3 \cdot T_1$ regardless of tip angle, so that the economy of a reduced tip angle is preserved at every level of accuracy.

The bias that arises in an integral ratio when the analyte and the internal standard relax at different rates has been quantified and tabulated at 30° and 90°. It is governed almost entirely by the slower of the two species, it is negative when the analyte is the slower, and a rigorous closed-form bound on the repetition time required to hold it inside a target has been given. Lengthening the delay, matching the relaxation time of the standard to that of the analyte, adding a paramagnetic relaxation agent, and external referencing have been identified as the available remedies.

The companion workbook returns the relaxation delay from the tip angle, the acquisition time and the relaxation time under the tolerance criterion, the multiple-of-T_1 rule and the Ernst condition side by side, together with the steady-state recovery, the signal attenuation, the sensitivity per unit time and the experiment duration; it evaluates a delay already chosen, and it solves the two-component bias problem against a target. In the worked example shipped with it, a 30° pulse with a 4 s acquisition time and a 5 s relaxation time requires a delay of 9.29 s for 1% recovery, against 21 s under the five-times-T_1 rule, at a cost in sensitivity per unit time of 0.44 relative to the fastest survey condition.

The tables are to be used with a relaxation time measured in the sample under the working conditions and on the instrument to be used, with a calibrated tip angle, and with dummy scans sufficient to establish the steady state; for heteronuclear work under inverse-gated decoupling the delay is extended to allow the residual Overhauser enhancement to decay, or a relaxation agent is used to remove the requirement. When these conditions are met, the relaxation delay read from the tables or returned by the workbook delivers the stated recovery, and the record of the parameters on the Calculator sheet constitutes the documentation that a quantitative result requires.